

## Microstructure and intergranular corrosion of the austenitic stainless steel 1.4970

Maysa Terada <sup>a</sup>, Mitiko Saiki <sup>a</sup>, Isolda Costa <sup>a,\*</sup>, Angelo Fernando Padilha <sup>b</sup>

<sup>a</sup> Instituto de Pesquisas Energéticas e Nucleares (IPEN/CNEN-SP) Av. Professor Lineu Prestes, 2242 Cidade Universitária, 05508-900 São Paulo (SP), Brazil

<sup>b</sup> Departamento de Engenharia Metalúrgica e de Materiais da Universidade de S. Paulo Av. Professor Mello Moraes, 2463, 05508-030 São Paulo (SP), Brazil

Received 9 November 2005; accepted 29 June 2006

### Abstract

The precipitation behaviour of the DIN 1.4970 steel and its effect on the intergranular corrosion resistance were studied. Time–temperature–precipitation diagrams for the secondary phases (Ti, Mo)C, (Cr, Fe, Mo, Ni)<sub>23</sub>C<sub>6</sub> and (Cr, Fe)<sub>2</sub>B are presented and representative samples have been selected for corrosion studies. The susceptibility to intergranular corrosion of the samples was evaluated using the double loop electrochemical potentiokinetic reactivation technique. The results showed that the solution-annealed samples and those aged at 1173 K did not present susceptibility to intergranular corrosion, whereas aging treatment from 873 to 1073 K resulted in small susceptibility to intergranular attack that decreased with aging temperature. The preferential formation of (Ti, Mo)C at higher aging temperatures comparatively to M<sub>23</sub>C<sub>6</sub>, retained the chromium in solid solution preventing steel sensitization and, consequently, intergranular corrosion.

© 2006 Elsevier B.V. All rights reserved.

### 1. Introduction

The titanium-stabilized full austenitic chromium–nickel steel DIN 1.4970 (15% Cr–15% Ni–1.2% Mo–Ti–B) was developed as a possible material for fast breeder sodium-cooled nuclear reactor core components [1]. More than 35 years research on this steel showed its superior creep strength [2,3], high microstructural stability [4–7] and elevated void swelling resistance [8,9]. Stabilizing element additions to austenitic stainless steels produce several

beneficial effects such as prevention of intergranular corrosion, reduction of void swelling and helium embrittlement, and precipitate strengthening [1]. The MC (M = Ti, Zr, Hf, V, Nb, Ta) carbides are very stable and are invariably present in stabilized austenitic stainless steels. The addition of elements that form MC carbides, called stabilizing elements, aims at hindering M<sub>23</sub>C<sub>6</sub> (M = Cr, Fe, Mo, Ni) precipitation and its associated undesirable consequences, particularly susceptibility to intergranular corrosion. On the other hand, systematic studies of intergranular corrosion on this steel were not found in the literature [1]. Intergranular corrosion is primarily due to grain boundary chromium depletion often coupled with other mechanisms supportive of

\* Corresponding author. Tel.: +55 11 3816 9356; fax: +55 11 3816 9370.

E-mail address: [icosta@ipen.br](mailto:icosta@ipen.br) (I. Costa).

Table 1  
Chemical composition (in wt%) of DIN 1.4970 stainless steel

C	Cr	Ni	Mo	Si	Mn	Ti	B	N	Fe
0.09	14.60	15.00	1.25	0.46	1.70	0.46	45 ppm	100 ppm	Balance

structural changes that lead to selective corrosion attack [10–13]. Sensitization in unstabilized austenitic stainless steels occurs in the temperature range between 753 and 1073 K and is caused by chromium carbide precipitation at grain boundaries and chromium depletion in adjacent regions. Furthermore, for stabilized austenitic stainless steels the critical temperature range is between 753 and 873 K due to the favored chromium carbide precipitation ( $M_{23}C_6$ ) in this temperature range [14,15].  $M_{23}C_6$  carbides have been found [16] in stabilized austenitic stainless steels in which the Ti/C mass ratio was as high as 34 when the stoichiometric ratio is only about 4. So, it is worthy of note that the addition of stabilizing elements does not entirely suppress precipitation of  $M_{23}C_6$ , even for large amounts of stabilizing elements [17]. For maximum intergranular corrosion resistance of stabilized austenitic grades, a heat treatment known as *stabilizing anneal*, that causes MC but no Cr-containing  $M_{23}C_6$  precipitation may be necessary. This treatment consists of heating the stainless steel in the range from 1118 to 1173 K, for up to 5 h, depending on the steel section thickness [18].

The precipitation behaviour of the 15% Cr–15% Ni–1.2% Mo–Ti–B austenitic stainless steel over prolonged periods of time (1000 h) in the temperature range from 873 to 1173 K was studied with the aid of various and complementary microstructural investigation techniques. This aging time was selected for the corrosion study because it was related to the larger number of  $M_{23}C_6$  precipitates. Initial results on time–temperature–precipitation (TTP) diagrams for the secondary phases [4–6] were analyzed in depth and representative samples have been selected for corrosion studies. The susceptibility to intergranular corrosion was evaluated with the double loop electrochemical potentiokinetic reactivation (DL-EPR) technique developed for austenitic stainless steels.

## 2. Experimental procedure

The chemical composition of the austenitic stainless steel (DIN 1.4970), used in this investigation was determined by several methods and is given in Table 1. The stainless steel used was solution

annealed at 1403 K for 30 min to dissolve chromium-containing carbide and boride precipitates [5]. Subsequently, aging treatments at various temperatures (873, 973, 1073 and 1173 K) were carried out for 1000 h. The stainless steel microstructures after solution annealing followed by various aging treatments were analyzed by optical microscopy (OM), scanning electron microscopy (SEM), energy dispersive X-ray element analysis (EDS), and transmission electron microscopy (TEM). The presence and amount of precipitates in the steel was evaluated by a phase separation technique that comprises selective dissolution of the matrix in a Berzelius-type solution, filtering and weighing of the precipitates, and finally their analysis by X-ray diffraction using a Guinier–Jagodzinski camera. A detailed description of the microstructural analysis procedures has been published elsewhere [4–6].

For evaluation of the susceptibility to intergranular corrosion, the surface of the steel was prepared by grinding with SiC paper #600. The specimens were then immersed in 2 m  $H_2SO_4$  + 0.5 m NaCl + 0.01 m KSCN solution at 303 K, and after 5 min immersion, the double loop electrochemical potentiokinetic reactivation (DL-EPR) method was employed. For this method, a three-electrode set-up cell was used, with a saturated calomel electrode (SCE) as the reference electrode, a platinum wire as the counter electrode and the specimen as the working electrode. All the potentials in this work are referred to the SCE electrode. In the DL-EPR method, the specimen was anodically polarized from the corrosion potential up to 500 mV (SCE) at a scan rate of 1.67 mV/s. At 500 mV, the polarization direction was reversed and the test was finished at the corrosion potential initially measured.

## 3. Results and discussion

Precipitation of various secondary phases such as carbides, sigma, chi and Laves phases can occur when austenitic stainless steels are exposed to elevated temperatures during aging heat treatments or service [17]. Minor amounts of these phases can have a major effect on the corrosion resistance of the stainless steels. Consequently, the knowledge of the amount, the distribution and the type of the

Table 2

Crystal structures and lattice parameters of the primary and secondary precipitates found in DIN 1.4970 stainless steel

Phase	Crystal structure	Lattice parameter (nm)
(Ti, Mo)C	fcc	$a = 0.43232$
Ti(N,C)	fcc	$a = 0.42517$
Ti <sub>4</sub> C <sub>2</sub> S <sub>2</sub>	hcp	$a = 0.32046$ ; $c = 1.12086$
(Cr, Fe, Mo, Ni) <sub>23</sub> C <sub>6</sub>	fcc	$a = 1.0645$
(Cr, Fe) <sub>2</sub> B	Orthorhombic	$a = 1.45583$ ; $b = 0.7379$ ; $c = 0.4245$

phases is critical to the corrosion properties of the stainless steels.

Five types of precipitates were identified in the DIN 1.4970 steel, as shown in Table 2. After solution annealing, three types of titanium bearing precipitates were identified: (Ti, Mo)C, Ti(N,C) and Ti<sub>4</sub>C<sub>2</sub>S<sub>2</sub>. Their average size was about 5 μm in diameter. While the carbides and sulphides were rounded, slightly elongated, the nitrides were faceted and roughly parallelepipedal. They were found intragranularly and at grain boundaries. To distinguish these precipitates from the others formed during the subsequent aging heat treatments, they will be called primary precipitates. After aging, three types of fine secondary precipitates were identified: (Ti, Mo)C, (Cr, Fe, Mo, Ni)<sub>23</sub>C<sub>6</sub> and (Cr, Fe)<sub>2</sub>B.

Fig. 1 shows the amount of precipitates (wt%) obtained in a previous work [5,6] from matrix dissolution followed by filtering, for specimens aged at increasing aging times and at several temperatures (873, 973, 1073 and 1173 K). Fig. 2 shows the time–temperature–precipitation diagram of this steel. Fig. 1 shows that the lowest amount of precipitates in the DIN 1.4970 stainless steel is associated with the specimen aged at 873 K, for the aging time

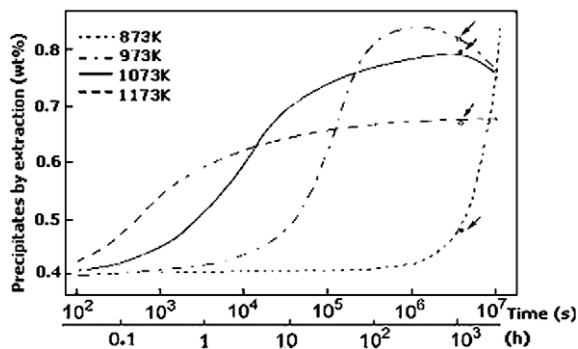


Fig. 1. Total amount of precipitates (wt%) extracted from DIN 1.4970 stainless steel solution annealed and aged at various temperatures as a function of aging time [5,6]. The arrows point to the samples used in this investigation (aging time of 1000 h).

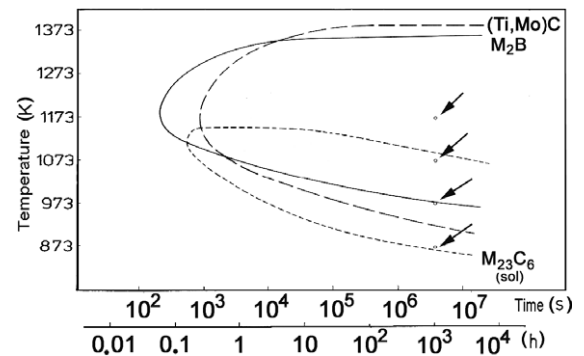


Fig. 2. Time–temperature–precipitation (TTP) diagrams for DIN 1.4970 stainless steel showing the precipitates related to aging temperature and time [5,6]. The arrows point to the samples used in this investigation (aging time of 1000 h). M<sub>23</sub>C<sub>6</sub> corresponds to (Cr<sub>13</sub>Fe<sub>7</sub>Mo<sub>2</sub>Ni<sub>1</sub>)C<sub>6</sub>, (Ti, Mo)C to (Ti<sub>0.9</sub>Mo<sub>0.1</sub>)C and M<sub>2</sub>B to (Cr<sub>1.65</sub>Fe<sub>0.35</sub>)B<sub>0.96</sub>.

used in this investigation (1000 h). The highest precipitates content, on the other hand, was found in the steel aged at 973 K and it decreased as the aging temperature increased from 973 to 1173 K. According to Fig. 2, the precipitates formed at 873 K for the aging time used in this investigation (1000 h) were mainly M<sub>23</sub>C<sub>6</sub>. In the temperature range from 973 to 1073 K, a larger variety of precipitates, such as (Ti<sub>0.9</sub>Mo<sub>0.1</sub>)C, (Cr<sub>13</sub>Fe<sub>7</sub>Mo<sub>2</sub>Ni<sub>1</sub>)C<sub>6</sub> and (Cr<sub>1.65</sub>Fe<sub>0.35</sub>)B<sub>0.96</sub> were formed, but at 1173 K, M<sub>23</sub>C<sub>6</sub> was not found.

The optical micrographs shown in Fig. 3 provide a general picture of the quantity and distribution of precipitates in the four investigated samples, nevertheless this technique does not allow the identification of each phase. The precipitates are both at grain boundaries and in grain interiors. However, the amount of precipitates inside the grains associated to the specimen aged at 873 K is lower than for the other specimens presented in Fig. 3(B)–(D). The TEM and SEM techniques were also used to investigate the microstructures and the results are shown in Figs. 4 and 5, respectively. For the steel specimens aged at 873 and 973 K, the precipitates identified were predominantly M<sub>23</sub>C<sub>6</sub> and these were mainly located at grain boundaries, whereas for the ones aged at 973, 1073 and 1173 K, (Ti, Mo)C were also found together with chromium carbides, not only inside the grains but also at the grain boundaries. (Cr, Fe)<sub>2</sub>B precipitates were additionally found chiefly at grain boundaries, but in very low amounts and are not expected to affect corrosion properties.

The σ, χ, Laves phase (Fe<sub>2</sub>Mo or Fe<sub>2</sub>Ti) and δ ferrite were not found even after prolonged

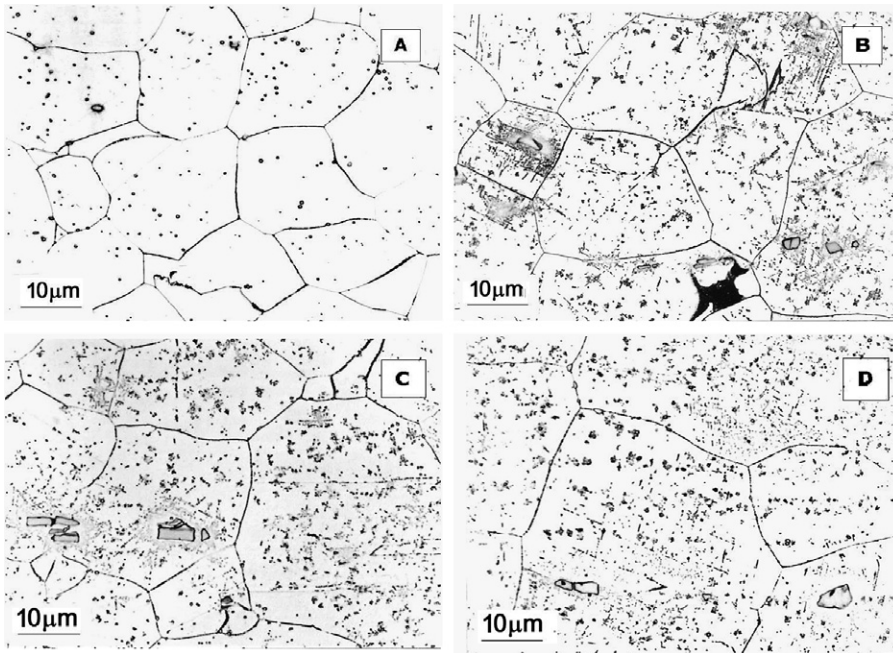


Fig. 3. Optical microscopy of DIN 1.4970 stainless steel solution annealed at 1403 K for 30 min and aged for 1000 h at (A) 873 K; (B) 973 K; (C) 1073 K; (D) 1173 K. See text for detailed explanation.

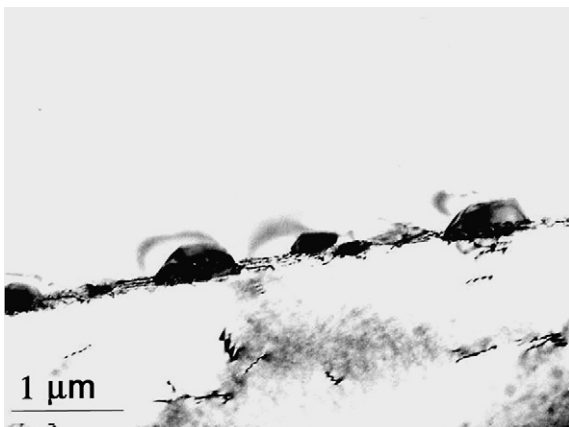


Fig. 4. Transmission electron micrograph of DIN 1.4970 stainless steel solution annealed and aged at 873 K for 1000 h, showing  $(Cr_{13}Fe_7Mo_2Ni_1)C_6$  at the grain boundaries.

high-temperature exposures. These phases often occur in similar austenitic stainless steels such as AISI 316 and 321 [17]. Increases in nickel and decreases in chromium content and well-adjusted molybdenum and titanium contents resulted in an alloy (DIN 1.4970) with improved microstructural stability, hindering  $\delta$  ferrite and strain induced martensites formation, as well as resistance against intermetallic phase precipitation during aging [17].

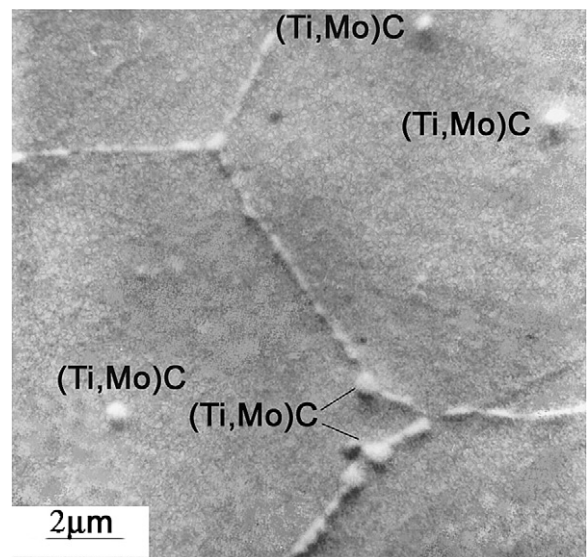


Fig. 5. Scanning electron micrograph of DIN W 1.4970 stainless steel solution annealed and aged at 973 K for 1000 h, showing  $(Cr_{13}Fe_7Mo_2Ni_1)C_6$  at the grain boundaries and  $(Ti_{0.9}Mo_{0.1})C$  – inside and at the grain boundaries.

The intergranular corrosion resistance of the DIN 1.4970 after the aging treatments was evaluated by the double loop electrochemical potentiokinetic reactivation technique (DL-EPR). This method is

based on the passivation followed by reactivation of the stainless steel surface from the passive state. The value of the maximum anodic current ( $i_a$ ) reached during the passivation stage is obtained from the polarization curve during the scan in the anodic direction. At 500 mV, the polarization direction is reversed, and if reactivation of the surface occurs, the maximum current during the reverse scan is the

Table 3

Values of  $i_r/i_a$  estimated from DL-EPR curves indicating susceptibility to intergranular corrosion of DIN 1.4970 austenitic stainless steel

DIN 1.4970 stainless steel	$i_r/i_a$
Solution-annealed at 1323 K for 30 min	–
Solution-annealed and aged at 873 K/1000 h	0.014
Solution-annealed and aged at 973 K/1000 h	0.008
Solution-annealed and aged at 1073 K/1000 h	0.0003
Solution-annealed and aged at 1173 K/1000 h	–

reactivation current ( $i_r$ ). For sensitized steels, reactivation occurs preferentially at the grain boundaries and the ratio ( $i_r/i_a$ ) indicates the susceptibility to intergranular corrosion.

The values of ( $i_r/i_a$ ) obtained from the DL-EPR method are shown in Table 3. The results indicated that both types of specimens, solution annealed and solution annealed and aged at 1173 K, did not present any susceptibility to intergranular corrosion. However, higher  $i_r/i_a$  values were associated to the former samples. The surface observation of this type of specimen suggested a more generalized type of attack on it. The aging treatment at 1173 K was the cause for the higher intergranular corrosion resistance of the latter samples. The heat treatment inside the stabilizing annealing temperature range (1118–1173 K) increased the corrosion resistance of the DIN 1.4970 steel [18]. For the specimens aged at temperatures from 873 to 1073 K, the resistance to intergranular corrosion increased with aging temperature. These results were due to the higher amount of  $M_{23}C_6$  precipitates associated to the steel aged at 873 comparatively to 1073 K, as

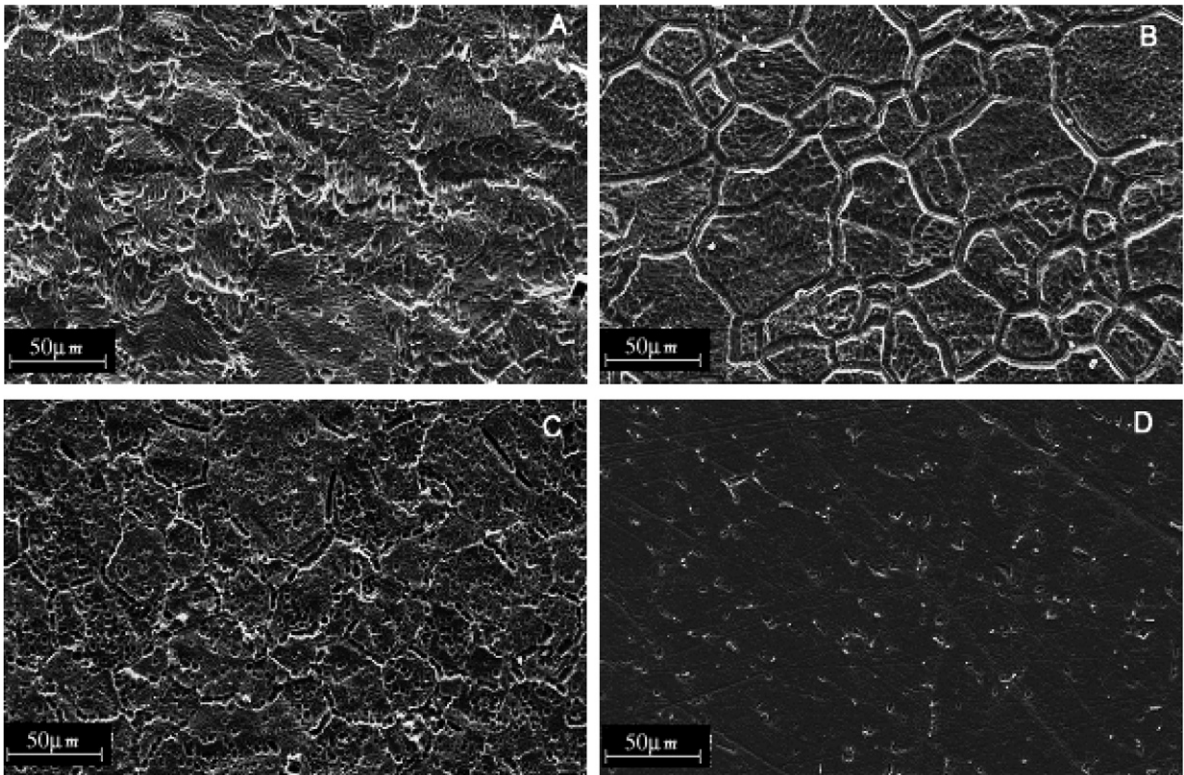


Fig. 6. Scanning electron micrographs of DIN 1.4970 stainless steel after the DL-EPR tests. (A) Solution-annealed; solution-annealed and aged for 1000 h at (B) 873 K; (C) 973 K; (D) 1173 K.

Table 4

Results of chemical analysis of test solution after DL-EPR tests carried out by instrumental neutron activation analysis (NAA)

Aging temperature (K)	Co ( $\mu\text{g mL}^{-1}$ )	Cr ( $\mu\text{g mL}^{-1}$ )	Fe ( $\mu\text{g mL}^{-1}$ )	Ni ( $\mu\text{g mL}^{-1}$ )
873	0.0121 $\pm$ 0.0004	2.013 $\pm$ 0.01	67.9 $\pm$ 0.5	14.4 $\pm$ 0.1
973	0.0041 $\pm$ 0.0005	1.973 $\pm$ 0.02	10.1 $\pm$ 2.1	1.8 $\pm$ 0.1
1073	0.0013 $\pm$ 0.001	2.213 $\pm$ 0.02	10.5 $\pm$ 0.3	2.2 $\pm$ 0.1
1173	*	0.533 $\pm$ 0.02	*	0.34 $\pm$ 0.05

\*Very low quantity.

suggested by the TTP diagrams shown in Fig. 2, and also to the increased Cr diffusion rate as the temperature increases. The increased diffusion rate decreases Cr concentration gradients around the  $M_{23}C_6$  precipitates and, consequently, reduces the degree of sensitization.

The results of the DL-EPR method supported those from the other analytical techniques used and the specimens that presented higher amounts of  $M_{23}C_6$  precipitates showed slight susceptibility to intergranular corrosion, whereas the (Ti,Mo)C precipitates had an opposite effect, increasing the steel intergranular corrosion resistance. This was due to the preferential formation of (Ti,Mo)C rather than  $M_{23}C_6$ , maintaining the chromium in solid solution and, consequently, preventing steel sensitization. After the DL-EPR tests, the specimens were observed by SEM and the micrographs obtained are shown in Fig. 6.

Analysis of the test solution after DL-EPR tests was carried out by instrumental neutron activation analysis (NAA) and the results are shown in Table 4. The quantities of Co, Fe and Ni were the highest in the solution where the sample aged at 873 K had been immersed. On the other hand, very similar Cr, Fe and Ni contents were found in the solutions where the samples aged at 973 and 1073 K had been exposed. The content of Cr in the solutions was in fact very similar for the samples aged from 873 to 1073 K. The minimum content of chemical elements in the test solution was associated to the sample aged at 1173 K, supporting the indication of increased intergranular corrosion resistance and corroborating the results of the other methods used in this study.

Titanium is added to the DIN 1.4970 steel (i) to avoid intergranular corrosion and (ii) to reduce irradiation induced swelling and creep by Ti–C precipitates in the matrix, which act as nucleation and recombination center for migration defects. This type of steel is frequently used [14,15] in the temperature range between 773 and 873 K and this is exactly the range of highest susceptibility to  $M_{23}C_6$

precipitation [5,6]. The results presented here clearly showed that the chromium carbide precipitates are the cause of susceptibility to intergranular corrosion and led to the conclusion that the addition of stabilizing elements does not suppress precipitation of  $M_{23}C_6$ , even when the stabilizers are present in large amounts [16]. In order to avoid sensitization, it is necessary to submit the steel, previous to its use, to a stabilizing heat treatment known as stabilizing anneal [18]. However, most favorable is a complementary cold working (cw) between the solution annealing and the stabilizing anneal, as the high dislocation density from cw acts as nucleation center for the formation of nano-sized Ti-containing precipitates that, in turn, are recombination centers for irradiation induced defects, thus suppressing very effectively the onset of the swelling threshold during high dose neutron irradiation [1].

#### 4. Conclusions

$M_{23}C_6$  precipitates were the predominant phases found at the grain boundaries of the solution-annealed and aged at 873 or 973 K (1000 h) DIN 1.4970 steel samples. These carbides were identified by X-ray diffraction, OM, SEM–EDS and TEM, and were also indicated by the TTP curves. Lesser amounts of these precipitates were found in the specimens aged at 1073 K but were not found in those aged at 1173 K. The increase in Cr diffusion with temperature resulted in lower concentration gradients around the  $M_{23}C_6$  precipitates and, consequently, in minor steel sensitization. In the specimens aged at 973, 1073 and 1173 K, (Ti,Mo)C precipitates were also found. The volume fractions of (Cr,Fe)<sub>2</sub>B precipitates were very low and did not affect the steel corrosion resistance. The preferential formation of (Ti,Mo)C at higher aging temperatures comparatively to  $M_{23}C_6$ , retained chromium in solution preventing steel sensitization and, consequently, intergranular corrosion. Analysis of the test solution after the DL-EPR experiment carried out by instrumental neutron activation

analysis showed that the solution-annealed specimens and those aged at 1173 K did not present a susceptibility to intergranular attack. The specimens aged at temperatures in the range from 873 to 1073 K showed a small susceptibility to intergranular attack that decreased with aging temperature. The results of the test solution analysis supported those obtained by the DL-EPR technique.

## References

- [1] H.-J. Bergmann, W. Dietz, K. Ehrlich, G. Mühling, M. Schirra, Forschungszentrum Karlsruhe, Report FZKA-6864, 2003.
- [2] G. Lagerberg, L. Egnell, Nucl. Eng. Int. 15 (1970) 203.
- [3] R.V. Nandedkar, W. Kesternich, Met. Trans. 21A (1990) 3033.
- [4] A.F. Padilha, G. Schanz, J. Nucl. Mater. 95 (1980) 229.
- [5] A.F. Padilha, Kernforschungszentrum Karlsruhe, Report KfK- 3151, 1981.
- [6] A.F. Padilha, G. Schanz, K. Anderko, J. Nucl. Mater. 105 (1982) 77.
- [7] W. Kesternich, D. Meertens, Acta Met. 34 (1986) 1071.
- [8] W. Schneider, C. Wassilew, K. Ehrlich, Z. Metallkunde 77 (1986) 611.
- [9] K. Ehrlich, Z. Metallkunde 94 (2003) 485.
- [10] C. Stawström, M. Hillert, J. Iron Steel Inst. 207 (1967) 77.
- [11] M. Pohl, H. Oppolzer, S. Schild, Mikrochim. Acta 10 (1983) 281.
- [12] E.P. Butler, M.G. Burke, Acta Met. 34 (1986) 557.
- [13] S.M. Brummer, Corrosion 44 (1988) 427.
- [14] M.J.G. Silva, A.A. Souza, A.V.C. Sobral, P. de Lima-Neto, H.F.G. Abreu, J. Mater. Sci. 38 (2003) 1009.
- [15] A.S. Lima, A.M. Nascimento, H.F.G. Abreu, P. de Lima-Neto, J. Mater. Sci. 40 (2005) 143.
- [16] L.K. Singhal, J.W. Martin, J. Iron Steel Inst. 205 (1967) 947.
- [17] A.F. Padilha, P.R. Rios, ISIJ Int. 42 (2002) 325.
- [18] ASM Handbook: Stainless steels. ASTM International, OH, USA, 1994, p. 291.